

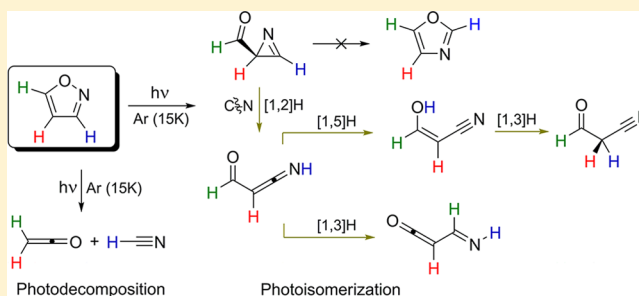
# UV-Laser Photochemistry of Isoxazole Isolated in a Low-Temperature Matrix

Cláudio M. Nunes,\* Igor Reva,\* Teresa M. V. D. Pinho e Melo, and Rui Fausto

Department of Chemistry, University of Coimbra, P-3004-535 Coimbra, Portugal.

**S** Supporting Information

**ABSTRACT:** The photochemistry of matrix-isolated isoxazole, induced by narrowband tunable UV-light, was investigated by infrared spectroscopy, with the aid of MP2/6-311+G(d,p) calculations. The isoxazole photoreaction starts to occur upon irradiation at  $\lambda = 240$  nm, with the dominant pathway involving decomposition to ketene and hydrogen cyanide. However, upon irradiation at  $\lambda = 221$  nm, in addition to this decomposition, isoxazole was also found to isomerize into several products: 2-formyl-2*H*-azirine, 3-formylketenimine, 3-hydroxypropenenitrile, imidoylketene, and 3-oxopropanenitrile. The structural and spectroscopic assignment of the different photoisomerization products was achieved by additional irradiation of the  $\lambda = 221$  nm photolyzed matrix, using UV-light with  $\lambda \geq 240$  nm: (i) irradiation in the  $330 \leq \lambda \leq 340$  nm range induced direct transformation of 2-formyl-2*H*-azirine into 3-formylketenimine; (ii) irradiation with  $310 \leq \lambda \leq 318$  nm light induced the hitherto unobserved transformation of 3-formylketenimine into 3-hydroxypropenenitrile and imidoylketene; (iii) irradiation with  $\lambda = 280$  nm light permits direct identification of 3-oxopropanenitrile; (iv) under  $\lambda = 240$  nm irradiation, tautomerization of 3-hydroxypropenenitrile to 3-oxopropanenitrile is observed. On the basis of these findings, a detailed mechanistic proposal for isoxazole photochemistry is presented.



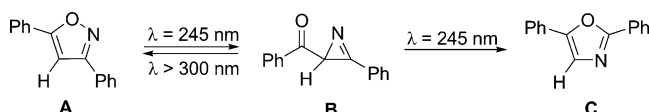
## 1. INTRODUCTION

Isoxazoles are an important class of five-membered unsaturated heterocyclic compounds. They show several applications in diverse areas such as pharmaceuticals, agrochemistry, and industry.<sup>1–5</sup> Isoxazoles are also found in natural sources showing insecticidal, plant growth regulation, and pigment functions.<sup>1–3</sup>

A structural feature that distinguishes isoxazoles from other heterocycles is the fact that its ring has properties of an aromatic system and, at the same time, has a weak N–O bond that plays a central role in their chemistry.<sup>1–3</sup> Indeed, under thermal or photochemical conditions, or even during the metabolism of several isoxazole-containing drugs, the N–O bond cleavage is described as the first step for their transformation.<sup>1–12</sup>

The earliest photochemical studies of isoxazoles were reported for 3,5-diphenylisoxazole **A** by Ullman and Singh in 1966 (Scheme 1).<sup>13</sup> This molecule shows an interesting

**Scheme 1. Photoisomerization of 3,5-Diphenylisoxazole A to 2,5-Diphenyloxazole C, via the 2-Benzoyl-3-phenyl-2*H*-azirine B Intermediate<sup>13</sup>**



photoisomerization reaction to 2,5-diphenyloxazole **C**. At  $\lambda = 245$  nm the reaction occurs through an initial ring contraction to yield the isolable 2-benzoyl-3-phenyl-2*H*-azirine **B**, which then undergoes ring expansion to **C**. On the other hand, irradiation of 2*H*-azirine **B** with longer wavelength ( $\lambda > 300$  nm) leads to photoreversion to isoxazole **A**.

The observed wavelength dependence was interpreted as selective excitation of one of two chromophores in 2*H*-azirine **B**.<sup>13–15</sup> The  $n,\pi^*$  excitation of the carbonyl chromophore that occurs at longer wavelengths should lead to the cleavage of the C–N bond, and formation of a diradical intermediate (vinylidene type), which recloses to isoxazole **A**. In contrast, the  $n,\pi^*$  excitation of the imine chromophore, promoted at shorter wavelengths, should lead to the cleavage of the C–C bond and formation of a zwitterionic intermediate (nitrile ylide type), which recloses to oxazole **C**.<sup>13–15</sup>

Studies on the photoisomerization of isoxazole **A** (and its aryl derivatives), using sensitizers, have not fully elucidated if the reported reaction involves triplet or singlet excited states.<sup>13–16</sup> Nevertheless, calculations on the potential energy surface (PES) of the parent isoxazole, at the MO-CI (STO-3G) ab initio level, indicate that the rearrangement to 2*H*-azirine occurs in a concerted manner, through the lowest singlet excited state ( $S_1$ ) of isoxazole.<sup>17</sup> The reverse reaction was

Received: August 9, 2012

Published: September 6, 2012

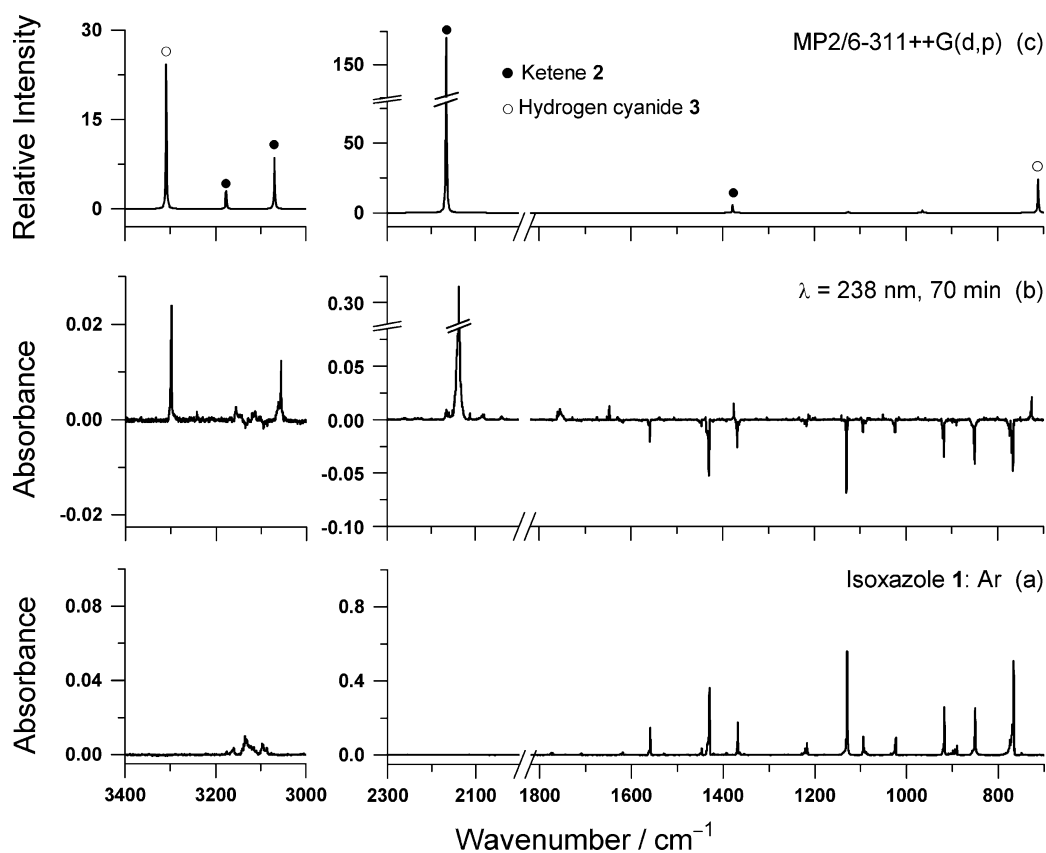


**Figure 1.** (a) Experimental IR spectrum of isoxazole **1** isolated in an argon matrix at 15 K. (b) Experimental difference spectrum; the spectrum obtained after UV-laser irradiation at  $\lambda = 238$  nm (70 min) of isoxazole **1** in argon matrix "minus" the spectrum of the sample before irradiation (as deposited). (c) Simulated IR spectra of ketene **2** (●) and hydrogen cyanide **3** (○) at the MP2/6-311++G(d,p) level, in ratio 1:1.

suggested to occur through the  $T_1$  triplet state, upon intersystem crossing from the  $S_1$  state of 2*H*-azirine. On the other hand, upon excitation of 2*H*-azirine to the  $S_2$  singlet excited state, C–C bond cleavage should occur, leading to oxazole formation.<sup>17</sup>

Further photochemical studies on several different substituted isoxazoles have established that isomerization to 2*H*-azirines, and then to oxazoles, is the most common pathway.<sup>18–32</sup> However, depending on the ring substitution pattern, or even on the solvent used, in some cases competitive reactions to nitriles or other species have also been observed.<sup>22–33</sup> In spite of these investigations, little is still known about the intermediates involved in the photochemical reactions of isoxazoles. Furthermore, no experimental results concerning the photochemical behavior of the simplest member of this family have been reported hitherto. Indeed, the photochemistry mechanism of isoxazoles is still far from being understood.

In this paper, we present the study of the photochemistry of the parent isoxazole using low-temperature matrix-isolation and infrared spectroscopy, complemented by quantum chemical calculations. Narrowband tunable UV-irradiation of the matrix-isolated isoxazole was undertaken in situ by means of an optical parametric oscillator (OPO) pumped by a pulsed Nd:YAG laser. The advantages provided by the cryogenic matrix environment, specifically the low temperature, inertness of the media, inhibition of molecular diffusion from the matrix cage, and high spectral resolution, make the used approach a powerful strategy for investigating the reaction intermediates and characterizing the reaction mechanisms involved in the

photochemistry of the studied compound. Here we reported previously unobserved UV-induced isoxazole ring-cleavage reactions and isomerizations, including various intramolecular hydrogen-atom shifts. The characterization of the photoproducts generated in these reactions allowed us to shed light, for the first time, on the complex photochemistry of the parent isoxazole.

## 2. RESULTS AND DISCUSSION

**Photochemistry of Isoxazole at  $\lambda = 238$  nm.** The photochemistry of monomeric isoxazole **1** isolated in an argon matrix was investigated using narrowband laser irradiation. A longer UV wavelength was first selected (300 nm) and then gradually decreased until changes in the sample, monitored by infrared spectroscopy, were observed. It was noticed that **1** starts to react, very slowly, upon UV-irradiation with  $\lambda = 240$  nm, whereas upon irradiation at  $\lambda = 238$  nm the same reaction goes slightly faster. Irradiations at 238 nm for 70 min consumed ~10% of **1**, and simultaneously, several new bands due to photoproducts appeared in the IR spectrum (Figure 1).

The new emerging band at 2137 cm<sup>-1</sup> was found to be at least 4 times more intense than the most intense band of **1** consumed. The frequency and high infrared intensity of this band allowed its easy assignment to the characteristic  $\nu(C=C=O)_{as}$  vibration of a ketene moiety.<sup>34</sup> In fact, observation of this very characteristic band, together with the bands appearing at 3056 and 1376 cm<sup>-1</sup>, allows unambiguous conclusion that this product is the parent ketene **2** [ $H_2C=C=O$ ]. In addition, hydrogen cyanide **3** [HCN], which is expected to be formed complementary to ketene **2** if

photodecomposition of isoxazole **1** occurs (Scheme 2), is identified by the observed bands at 3300 and 727/725  $\text{cm}^{-1}$

**Scheme 2. Dominant Photochemical Reaction of Isoxazole 1 Isolated in an Argon Matrix upon UV-Laser Irradiation at  $\lambda = 238 \text{ nm}$**

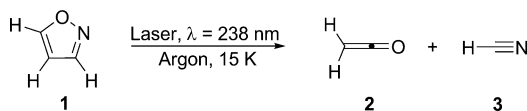


(Figure 1). These bands correspond to the  $\nu(\text{C-H})$  and  $\delta(\text{HCN})$  vibrations of HCN, respectively (see Supporting Information (SI), Table S1).

When the current IR data are compared with the data reported for matrix isolated monomeric **2**<sup>35–37</sup> and **3**,<sup>38,39</sup> a shift of 5  $\text{cm}^{-1}$  in frequencies is observed (Table S1, SI), suggesting that ketene **2** and hydrogen cyanide **3**, produced from isoxazole **1**, form a complex in the same matrix cage. This hypothesis is also supported by the excellent agreement between the present results and those corresponding to the reported UV photochemistry of acetyl cyanide [ $\text{CH}_3\text{COCN}$ ] in an argon matrix, where formation of complexes of **2** and **3** was described (Table S1, SI).<sup>40</sup>

**Photochemistry of Isoxazole at  $\lambda = 221 \text{ nm}$ .** When isoxazole **1** isolated in an argon matrix was irradiated at shorter wavelengths, different results were obtained. Upon irradiation at  $\lambda = 221 \text{ nm}$ , the shortest wavelength available in our (UV-laser + OPO) system, many additional photoproduct bands, besides those corresponding to **2** and **3**, were observed (Figure 2). In these conditions, after one minute of irradiation more than 10% of **1** was consumed. The most intense new bands, which emerged in the 2100–2000  $\text{cm}^{-1}$  and 1800–1600  $\text{cm}^{-1}$

regions, are due to the formation of several photoisomerization products labeled with numbers **4** to **8** (Figure 2b). As will be shown below, their identification was achieved with the aid of subsequent irradiation experiments using longer wavelengths ( $\lambda \geq 240 \text{ nm}$ ), i.e., under conditions where the parent isoxazole is photostable.

**Identification of Isoxazole Photoisomerization Products Generated at  $\lambda = 221 \text{ nm}$ .** The UV-laser irradiation at  $\lambda = 221 \text{ nm}$  was applied to isoxazole **1** isolated in an argon matrix until a maximum yield of photoisomerization products was achieved (which corresponded to  $\sim 60\%$  consumption of **1**).<sup>41</sup> Subsequently, the matrix was further irradiated using UV-light within the 340–240 nm region, starting with longer wavelengths, which were then gradually decreased while changes were monitored by FTIR spectroscopy. These irradiation experiments allowed the observation of individual reactions of the products **4** to **8**, while the isoxazole **1** remained intact. The results presented below correspond to the most illustrative and spectacular observed changes, which were selected to demonstrate consumption of different photoisomerization products and permit their unequivocal assignment. The actual number of the irradiations performed, in the course of the reported experiments, was quite large to guarantee that as many as possible different photoreactions, occurring upon excitation at different UV-thresholds, are characterized (see SI, Table S2).

**Irradiation Experiments in the  $330 \leq \lambda \leq 340 \text{ nm}$  Range.** The irradiation within the  $330 \leq \lambda \leq 340 \text{ nm}$  range,<sup>42</sup> of the photoisomerization products of isoxazole **1** isolated in an argon matrix, led to the production of 3-formylketenimine **5** and consumption of the isomeric 2-formyl-2H-azirine **4** (Figure 3 and Scheme 3).<sup>43</sup> The bands that increased in the IR spectrum, observed at 2042, 1703 (also labeled with **5** in Figure 2b), and

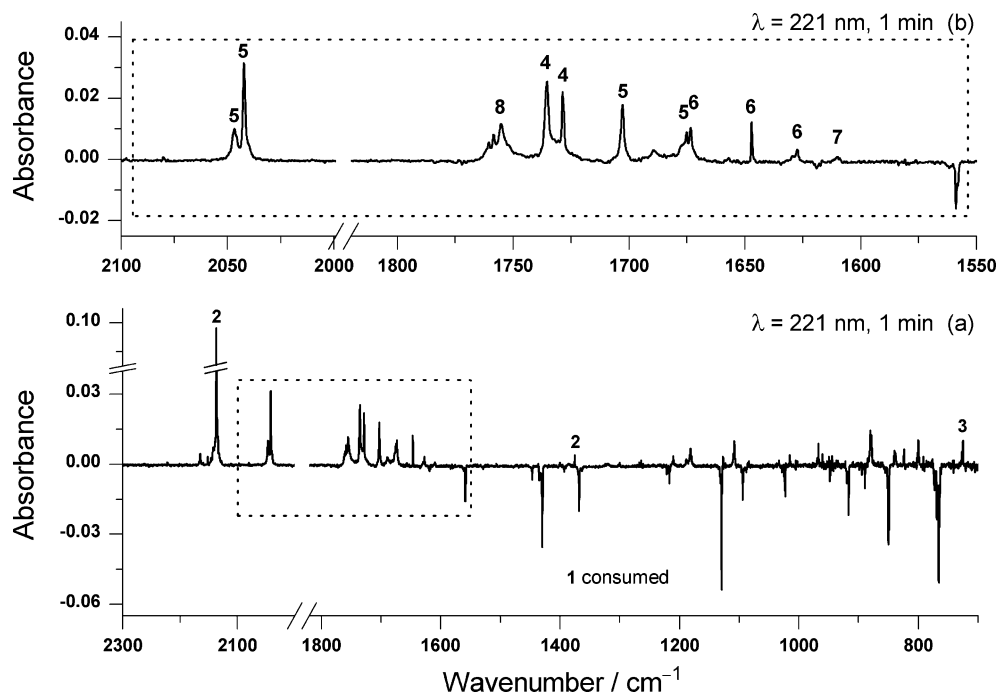


**Figure 2.** (a) Experimental difference IR spectrum; the spectrum obtained after UV-laser irradiation at  $\lambda = 221 \text{ nm}$  (1 min) of isoxazole **1** in argon matrix “minus” the spectrum of the sample before irradiation (as deposited). Positive labeled bands are due to ketene **2** and hydrogen cyanide **3**. (b) Expanded view, corresponding to the dashed rectangle in frame (a), showing only the 2100–2000  $\text{cm}^{-1}$  and 1800–1600  $\text{cm}^{-1}$  regions, where the most intense bands due to photoisomerization products (labels **4** to **8**) appear (see text).

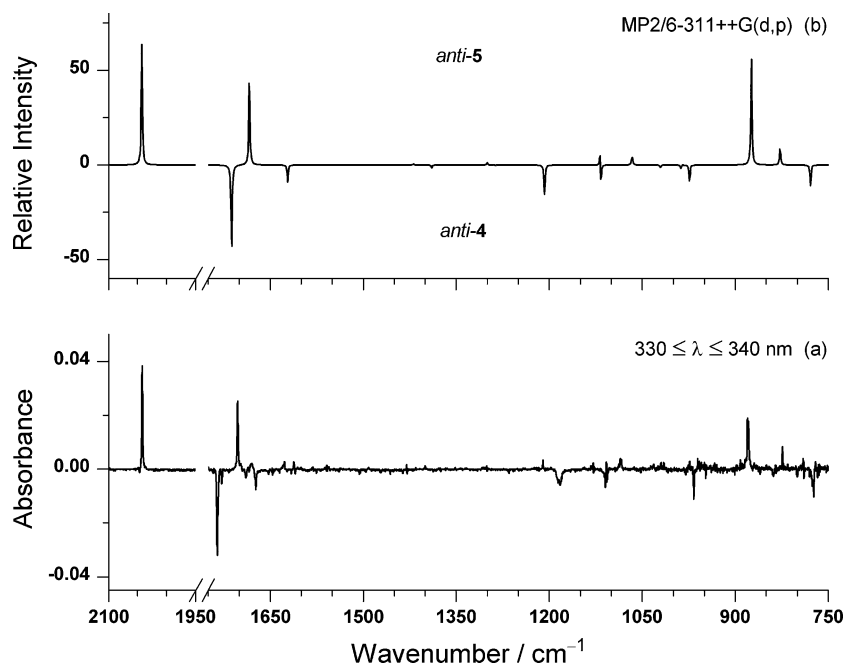
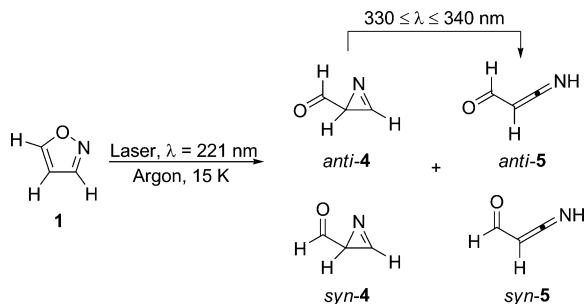


**Figure 3.** (a) Experimental difference IR spectrum; the spectrum obtained after UV-laser irradiation of photoisomerization products of isoxazole **1** in an argon matrix, in the  $330 \leq \lambda \leq 340$  nm range (10 min), “minus” the spectrum before this irradiation, corresponding to the photoisomerization products of isoxazole **1** produced at  $\lambda = 221$  nm (see text). (b) Simulated difference IR spectrum at the MP2/6-311++G(d,p) level considering the production of ketenimine *anti*-5 (positive bands) and the consumption of 2*H*-azirine *anti*-4 (negative bands).

**Scheme 3. Identification of 2-Formyl-2*H*-azirine **4** and 3-Formylketenimine **5** as Photoisomerization Products of Isoxazole **1** ( $\lambda = 221$  nm), by Means of Subsequent Irradiation Experiments in the  $330 \leq \lambda \leq 340$  nm Range**



$880\text{ cm}^{-1}$ , are reliably assigned to ketenimine **5**, namely, to its characteristic  $\nu(\text{C}=\text{C}=\text{N})_{\text{as}}$ ,  $\nu(\text{C}=\text{O})$ , and  $\delta(\text{HNC})$  vibrational modes, respectively (see also Table S3, SI). At the same time, the bands that decreased in the spectrum, observed at  $2824$ ,  $1735$  (also labeled with **4** in Figure 2b),  $1673$ , and  $1186/1182\text{ cm}^{-1}$ , are ascribed to 2*H*-azirine **4**, more specifically to its  $\nu(\text{CHO})$ ,  $\nu(\text{C}=\text{O})$ ,  $\nu(\text{C}=\text{N})_{\text{ring}}$  and  $\nu(\text{C}-\text{C})_{\text{ring}}$  vibrational modes, respectively (see also Table S4, SI). These conclusions are unequivocally established by the excellent correlation between the experimental and the MP2/6-311++G(d,p) calculated difference IR spectra (Figure 3).

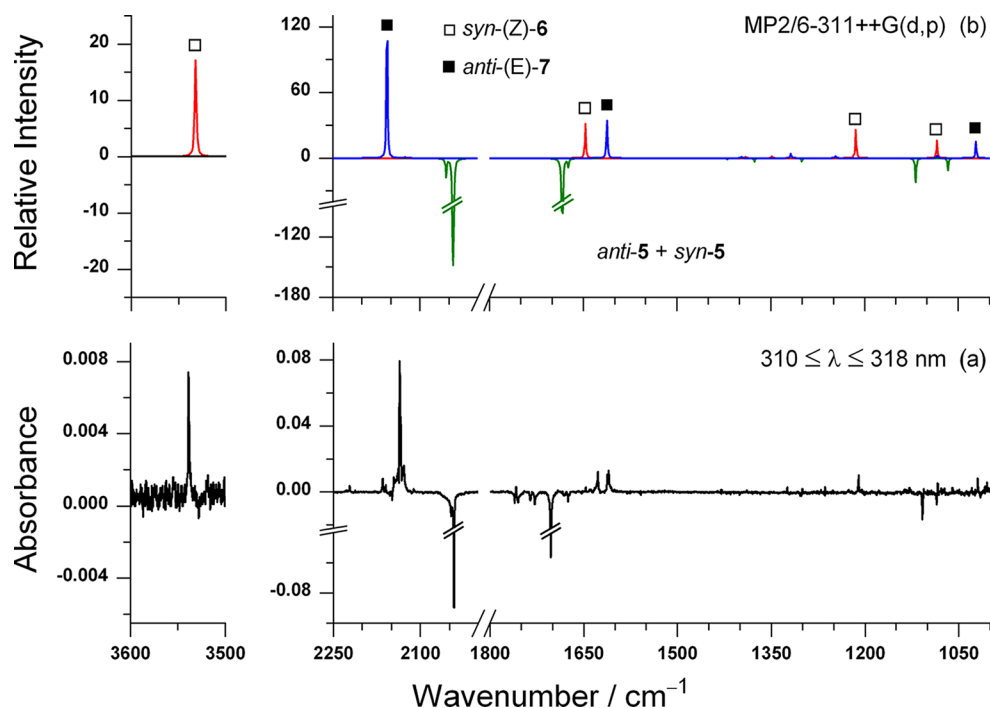
Calculations on the PES of **4** and **5** show that both molecules have two different conformations, *syn* and *anti*, with the *anti* forms being more stable by  $4\text{--}5\text{ kJ mol}^{-1}$  (Figures S2 and S3, SI). As presented in Figure 3, the irradiation in the  $330 \leq \lambda \leq 340$  nm range led mainly to the photoreaction of the *anti*-4 form to give the *anti*-5 form. However, the *syn* forms of 2*H*-azirine **4** and ketenimine **5** could also be identified as photoisomerization products of isoxazole **1** at  $\lambda = 221$  nm. In

Figure 2b, the lower-frequency band labeled with **4**, observed at  $1728\text{ cm}^{-1}$ , is assigned to the *syn*-4 conformer (the higher-frequency band labeled with **4**, at  $1735\text{ cm}^{-1}$ , is due to *anti*-4, as previously indicated); additional data are presented in Table S4 (SI). In the case of the *syn*-5 conformer, its identification is mainly established based on the minor observed bands, labeled with **5** in Figure 2b, that appear at  $2047\text{ cm}^{-1}$  [ $\nu(\text{C}=\text{C}=\text{N})_{\text{as}}$ ] and  $1680/1675\text{ cm}^{-1}$  [ $\nu(\text{C}=\text{O})$ ] (see also Table S3, SI).

**Irradiation Experiments in the  $310 \leq \lambda \leq 318$  nm Range.** After the consumption of 2-formyl-2*H*-azirine **4**, further irradiation conducted in the  $318\text{--}310$  nm range led to the consumption of 3-formylketenimine **5** concomitantly with the increase of several bands (Figure 4a). From the analysis of the spectral changes, 3-hydroxypropenenitrile *syn*-(*Z*)-**6** (the most stable of four conformers, Figure S4, SI) could be easily identified. For example, the bands at  $3538$ ,  $2221$ , and  $1627\text{ cm}^{-1}$  (also labeled with **6** in Figure 2b) correlate well with the reported IR data for this species,<sup>9</sup> namely, its  $\nu(\text{O}-\text{H})$ ,  $\nu(\text{C}\equiv\text{N})$ , and  $\nu(\text{C}=\text{C})$  characteristic bands, respectively (see Table S5, SI).

Furthermore, the formation of the imidoalkene *anti*-(*E*)-**7** (the most stable of four conformers, Figure S5, SI) could also be unambiguously established. The band observed at  $2136/2134\text{ cm}^{-1}$  appears in the characteristic region of the  $\nu(\text{C}=\text{C}=\text{O})_{\text{as}}$  vibration of imidoalkenes isolated in the low-temperature matrix.<sup>44–53</sup> In addition, the bands observed at  $1612/1610\text{ cm}^{-1}$  (also labeled with **7** in Figure 2b) and  $1020\text{ cm}^{-1}$  show an excellent correlation with the most intense bands estimated at the MP2/6-311++G(d,p) level for *anti*-(*E*)-**7**, namely, those predicted at  $1612\text{ cm}^{-1}$  [ $\nu(\text{N}=\text{C})$ ] and  $1022\text{ cm}^{-1}$  [ $\delta(\text{HNC}) + \nu(\text{C}-\text{C})$ ].

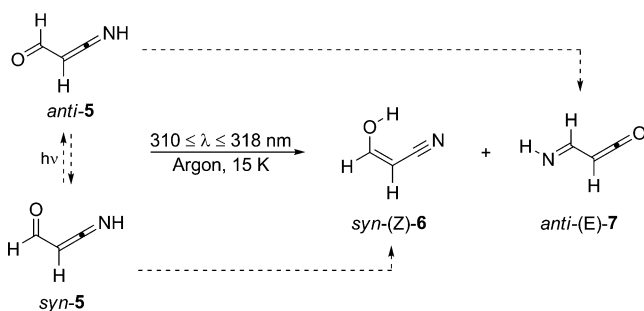
The MP2/6-311++G(d,p) calculated difference IR spectrum, considering the consumption of *syn*-**5** and *anti*-**5** (0.1:1) and formation of *syn*-(*Z*)-**6** and *anti*-(*E*)-**7** (0.6:0.5) (Figure 4b), shows an excellent agreement with the experimental difference



**Figure 4.** (a) Experimental difference IR spectrum; the spectrum obtained after UV-laser irradiation, in the  $310 \leq \lambda \leq 318$  nm range (25 min), “minus” the spectrum previous to this laser irradiation, after the consumption of **4** (see text). (b) Calculated IR spectra at the MP2/6-311++G(d,p) level considering the production of hydroxynitrile *syn*-(Z)-**6** (red line, □) and imidoylketene *anti*-(E)-**7** (blue line, ■) (0.6:0.5) and the consumption of ketenimine *syn*-**5** and *anti*-**5** (0.1:1) (green line, negative bands).

IR spectrum (Figure 4a), strongly supporting the structural assignments (Scheme 4).

**Scheme 4. Identification of 3-Hydroxypropenenitrile *syn*-(Z)-**6** and Imidoylketene *anti*-(E)-**7** as Photoisomerization Products of Isoxazole **1** ( $\lambda = 221$  nm), by Means of Subsequent Irradiation Experiments in the  $310 \leq \lambda \leq 318$  nm Range, That Lead to Their Formation from the Consumption of 3-Formylketenimine **5****



**Irradiation Experiments in the  $240 \leq \lambda \leq 280$  nm Range.** After consumption of 2*H*-azirine **4** and ketenimine **5** in the course of  $300 \leq \lambda \leq 340$  nm irradiation, it was observed that further irradiation with  $\lambda = 280$  nm led to the reaction of another species, which could be identified as 3-oxopropanenitrile **8**. Although other transformations seem also to occur, under these conditions the main process was consumption of the *anti*-**8** conformer (the most stable form of **8**, Figure S6, SI). This is clearly supported by the good agreement between the experimental difference IR spectrum and the MP2/6-311++G(d,p) calculated data (Figure 5).

The two most intense bands in the experimental spectrum observed at  $1760/1758/1755$   $\text{cm}^{-1}$  (also labeled with **8** in Figure 2b) and at  $1020/1015$   $\text{cm}^{-1}$  are in good agreement with those estimated at  $1729$   $\text{cm}^{-1}$  [ $\nu(\text{C}=\text{O})$ ] and at  $1032$   $\text{cm}^{-1}$  [ $\nu(\text{OC}-\text{C})$ ] for *anti*-**8**.<sup>54</sup> In addition, the two bands observed at  $1400$  and  $1384$   $\text{cm}^{-1}$  could be assigned to the  $\delta(\text{CH}_2)$  and  $\delta(\text{OCH})$  bending modes of *anti*-**8**, calculated at  $1424$  and  $1394$   $\text{cm}^{-1}$ , respectively.

Simultaneously with the consumption of the ketonitrile **8**, the bands at  $2292$  and at  $2257$   $\text{cm}^{-1}$  were observed to increase. These bands are characteristic of acetonitrile.<sup>55–57</sup> Although the appearance of the band due to CO ( $\sim 2138$   $\text{cm}^{-1}$ )<sup>58,59</sup> is difficult to establish with certainty, due to the overlap with the much more intense bands of ketenes **2** and **7**, the formation of CO together with acetonitrile could indicate a potential photodecomposition channel for **8**.

After consumption of ketonitrile **8** (and also imidoylketene **7**, that disappear during subsequent irradiations with  $280$ – $250$  nm; see also SI, Table S2), irradiation experiments in the  $248$ – $244$  nm region led to the *Z*  $\rightarrow$  *E* photoisomerization of the hydroxynitrile **6** (Figure 6). This result is in accordance with reported results from previous experiments performed under similar conditions (see Table S5, SI).<sup>9</sup> On the basis of these data, the bands labeled with **6** in Figure 2b, observed at  $1673$ ,  $1647$ , and  $1627$   $\text{cm}^{-1}$ , are reliably assigned to the  $\nu(\text{C}=\text{C})$  of *anti*-(E)-**6**, *syn*-(E)-**6**, and *syn*-(Z)-**6**, respectively (the hydroxynitrile *syn*-(Z)-**6** was also identified during irradiation experiments in the  $310 \leq \lambda \leq 318$  nm range, as already mentioned).

Finally, irradiation experiments with  $\lambda = 240$  nm (under these conditions isoxazole **1** reacts negligibly slow) led to the consumption of different conformers of hydroxynitrile **6** and to formation of ketonitrile **8** (Figure 7). The phototautomerization **6**  $\rightarrow$  **8** is undoubtedly identified by considering, for



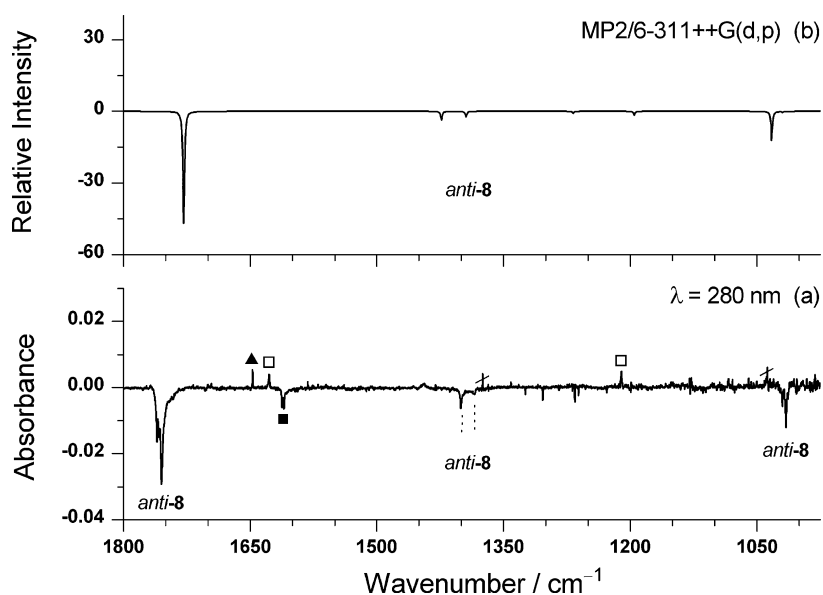


**Figure 5.** (a) Experimental difference IR spectrum; the spectrum obtained after UV-laser irradiation at  $\lambda = 280$  nm (30 min) “minus” the spectrum previous to this laser irradiation, after the consumption of 4 and 5 (see text). Bands labeled with (▲) and (□) are due to *syn*-(E)-6 and *syn*-(Z)-6, and that labeled with (■) is due to *anti*-(E)-7. (b) Simulated difference IR spectrum at the MP2/6-311++G(d,p) level considering the consumption of ketonitrile *anti*-8.

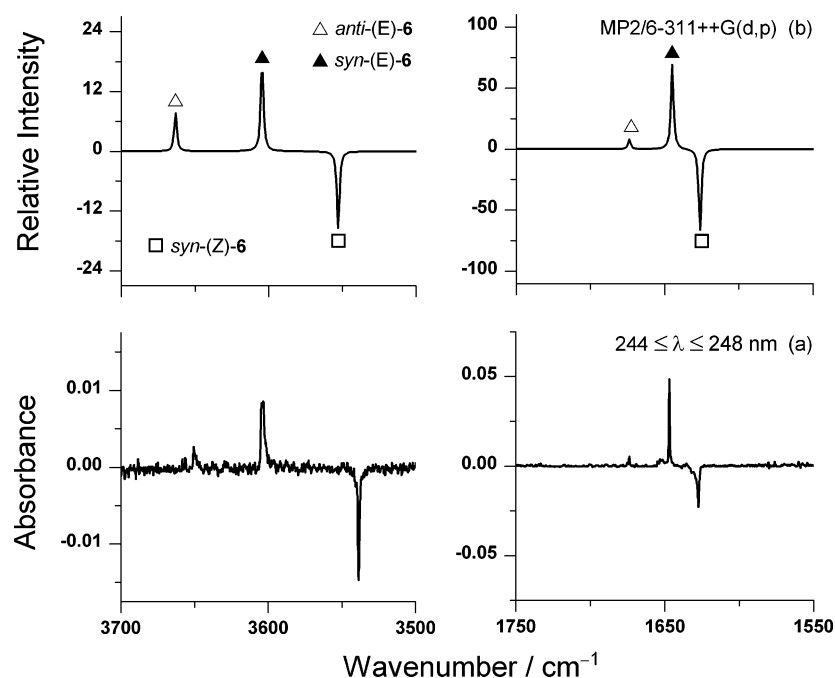


**Figure 6.** (a) Experimental difference IR spectrum; the spectrum obtained after UV-laser irradiation, in the  $244 \leq \lambda \leq 248$  nm range (11 min), “minus” the spectrum previous to this laser irradiation, after the decomposition of imidoylketene 7 and ketonitrile 8 (see text). (b) Simulated difference IR spectrum at the MP2/6-311++G(d,p) level considering the photoisomerization of hydroxynitrile *syn*-(Z)-6 (□) (negative bands) to *syn*-(E)-6 (▲) and *anti*-(E)-6 (△) (positive bands) in a ratio of 0.85:0.15.

example, the decrease of the bands at 1627, 1647, and 1673  $\text{cm}^{-1}$  (due to the  $\nu(\text{C}=\text{C})$  of *syn*-(Z)-6, *syn*-(E)-6, and *anti*-(E)-6, respectively) and the concomitant increase of the band at 1760/1758/1755  $\text{cm}^{-1}$ , corresponding to  $\nu(\text{C}=\text{O})$  of *anti*-8 (identified also during irradiation experiments at  $\lambda = 280$  nm and labeled with 8 in Figure 2b). The summary of the irradiation experiments in the  $240 \leq \lambda \leq 280$  nm range is presented in Scheme 5.

**Mechanism of the Photochemistry of Isoxazole.** The summary of the experimental results together with a mechanistic proposal for the photochemistry of parent isoxazole 1 are presented in Scheme 6. Irradiations within the  $238 \leq \lambda \leq 240$  nm range (the longest wavelengths that induce reaction of 1) led mainly to the hitherto unobserved photodecomposition of 1 to ketene 2 and hydrogen cyanide 3. One may suppose that this reaction occurs via an isoxazole carbene tautomer, formed by a [1,2] sigmatropic H-shift from

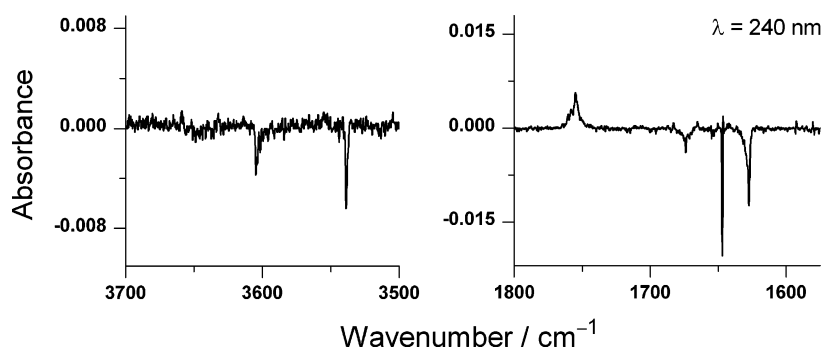
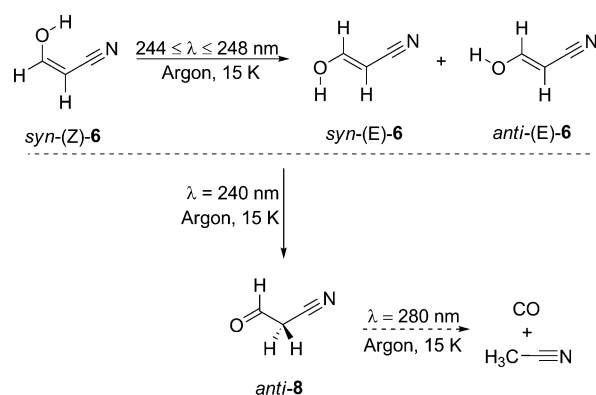


**Figure 7.** Experimental difference IR spectrum showing the phototautomerization  $6 \rightarrow 8$ ; the spectrum obtained after UV-laser irradiation at  $\lambda = 240$  nm (6 min) “minus” the spectrum previous to this laser irradiation, after the  $Z \rightarrow E$  photoisomerization of hydroxynitrile **6** (see text).

**Scheme 5. Identification of 3-Hydroxypropenenitrile *syn*-(Z)-**6**, *syn*-(E)-**6**, and *anti*-(E)-**6**, and 3-Oxopropanenitrile *anti*-**8** as Photoisomerization Products of Isoxazole **1** ( $\lambda = 221$  nm), by Means of Subsequent Irradiation Experiments in the  $240 \leq \lambda \leq 280$  nm Range**



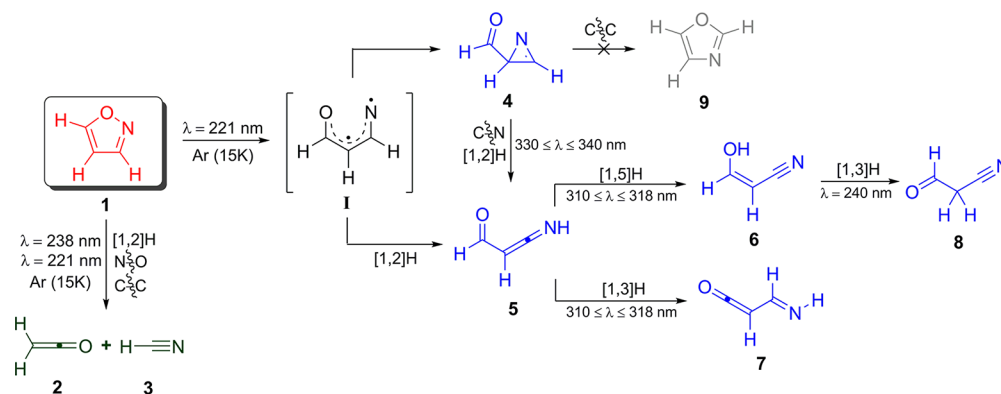
C5 to C4, which could then decompose through the cleavage of the weakest N–O and C4–C3 bonds.<sup>9</sup> However, since no intermediates were detected during the experiments in argon matrices at 15 K, the establishment of the definitive mechanism for this new photodecomposition reaction still requires further investigation.

When the irradiation of isoxazole **1** was performed with shorter wavelengths, namely, at  $\lambda = 221$  nm, the new photoisomerization products, 2*H*-azirine **4**, ketenimine **5**,

hydroxynitrile **6**, imidoylketene **7**, and ketonitrile **8**, were also observed. Contrary to what could be expected, no photoisomerization to oxazole **9** was detected.<sup>60</sup> Since the bands due to 2*H*-azirine **4** and ketenimine **5** reach their maxima in the first minutes (while the bands of the other photoisomerization products reach their maxima somewhat later, Figure S1, SI), it can be suggested that **4** and **5** are primary isomerization products in the isoxazole **1** photochemistry.

Recently, we reported that vinylnitrene **I**, which results from the cleavage of the N–O bond, is a very reactive minimum on the PES of isoxazole **1**.<sup>9</sup> Although its existence remains yet to be experimentally proven, this species is probably an intermediate in the photochemistry of **1** that gives rise to the formation of 2*H*-azirine **4** and ketenimine **5**. Under this hypothesis, it is likely that the open-shell singlet vinylnitrene **I**, better described as a 1,3-diradical, collapses easily once formed to give the 2*H*-azirine **4** (as reported in ref 9; this is the lowest-energy deactivation path and requires only the movement of the nitrogen atom out of the molecular plane and the closure of the N–C–C angle).<sup>9,61–63</sup> On the other hand, it can conceivably be hypothesized that the ground-state triplet vinylnitrene **I**, in which the amount of delocalization of the nonbonding  $\pi$  electron from nitrogen is expected to be modest,<sup>9,61–63</sup> is responsible for the formation of ketenimine **5** through a [1,2] sigmatropic H-shift reaction (vide infra; in addition it should be noted that triplet ground states of aryl nitrenes are known to be reactive as hydrogen-atom abstracting agents<sup>64–66</sup>).

**Scheme 6. Summary of Experimental Observations and the Mechanistic Proposal for the UV-Induced Photochemistry Pathways of Isoxazole **1** Isolated in a Low-Temperature Argon Matrix<sup>a</sup>**



<sup>a</sup>Structures given in blue possess different conformers (for simplicity not shown).

In the irradiation experiments of photoisomerization products of isoxazole **1**, it was observed that 2-formyl-2H-azirine **4** is converted into 3-formylketenimine **5** when irradiated in the  $330 \leq \lambda \leq 340$  nm range. Some examples of the unusual photochemical cleavage of the C–N bond in 2H-azirines, to give rise to ketenimines, have been reported.<sup>67–71</sup> This reaction is mainly observed when longer irradiation wavelengths are used, but even in these apparently exceptional cases the common C–C bond cleavage also occurs (at least with lower irradiation wavelengths).<sup>67–71</sup> On the basis of different experimental data, Inui and Murata proposed that the cleavage of the C–N bond of 2H-azirines involves the formation of a vibrationally excited triplet vinylnitrene, which then undergoes Curtius-like rearrangement to the corresponding ketenimines.<sup>69,72</sup> These results are consistent with our hypothesis, where it is suggested that triplet vinylnitrene **I**, formed from isoxazole **1** via N–O bond cleavage (or from 2H-azirine **4**), is an intermediate in formation of ketenimine **5**.

The nonexistence of photoisomerization to oxazole **9** indicates that during irradiation 2H-azirine **4** does not react via C–C bond cleavage. Only the C–N bond cleavage of **4** should exclusively occur, even when lower wavelengths are used, which made this derivative a special case in the photochemistry of 2H-azirines (results that surely deserve future investigations).

Subsequently, irradiation experiments with  $310 \leq \lambda \leq 318$  nm led to the interesting photoisomerization of 3-formylketenimine **5** to hydroxynitrile **6** and imidoylketene **7**. This reaction must be conformer-selective; i.e., the *syn*-**5** leads to *syn*-(*Z*)-**6** through a [1,5] sigmatropic H-shift (the only conformer identified), whereas the *anti*-**5** gives rise to *anti*-(*E*)-**7** through a [1,3] sigmatropic H-shift (also the only conformer identified) (see also Scheme 4). However, the ratio of *syn*-**5**:*anti*-**5** before irradiation (~0.1:1) does not match the ratio of products *syn*-(*Z*)-**6**:*anti*-(*E*)-**7** formed after the irradiation (~0.6:0.5). This fact could be due to the existence, during the irradiation process, of facile photoisomerization between *syn*-**5** and *anti*-**5** (several examples of isomerizations of aldehydes of this type, during the UV-irradiation, are known<sup>73,74</sup>). To the best of our knowledge, the phototransformation of 3-formylketenimine is reported for the first time herein. The [1,5] sigmatropic H-shift reaction of ketenimines to give hydroxynitrile derivatives was only suggested in the literature as a thermally induced reaction to explain the results of the study of flash vacuum pyrolysis (FVP) matrix-isolation of pyrrolidone derivatives, namely, the conversion of the imidoylketene derivatives (primary products) to the isomeric nitriles (final products).<sup>52</sup> The [1,3] sigmatropic H-shift reaction of ketenimines to give imidoylketenes (or the corresponding reverse isomerization) is, on the other hand, a better known thermal reaction described in several FVP matrix-isolation studies.<sup>47–52</sup>

Finally, the formation of ketonitrile **8** was observed to occur through phototautomerization of hydroxynitrile **6**, based on the results of irradiation experiments with  $\lambda = 240$  nm of isoxazole **1** photoproducts. This observation is not completely unexpected since the existence of thermal tautomeric equilibrium between these species (with their ratio being dependent on the solvent used) was already reported in the FVP study of a Meldrum's acid derivative.<sup>46</sup> Furthermore, in our previous reported study on the thermal reactivity of isoxazoles, the possibility that this reaction takes place was also suggested based on experimental and theoretical results.<sup>9</sup>

In some particular cases, the photoisomerization of isoxazoles into ketonitriles has been previously reported.<sup>32</sup> The results from the current study indicate that this reaction should take place preferentially with 5-unsubstituted isoxazoles, since the [1,5] sigmatropic H-shift from ketenimine to hydroxynitrile is not blocked by substituents, and the subsequent phototautomerization to ketonitriles can occur. In fact, the detailed mechanism for a ketonitrile formation upon irradiation of isoxazole was established in this study for the first time.

### 3. CONCLUSION

Use of matrix isolation infrared spectroscopy and in situ narrowband tunable UV irradiation of matrix-isolated parent isoxazole allowed us for the first time to establish a detailed picture of the unimolecular photochemistry of this compound. The experimental studies received support from MP2/6-311++G(d,p) theoretical calculations of the structure and spectra of the relevant species.

Isoxazole was found to be photostable upon UV irradiation with  $\lambda > 240$  nm. Upon irradiation of the matrix-isolated compound at  $\lambda = 240$ –238 nm, the dominant observed photoreaction was isoxazole decomposition to ketene and hydrogen cyanide. On the other hand, irradiation at  $\lambda = 221$  nm was found to induce additionally a series of isomerization processes that led to formation of several products, which could be identified by additional photochemical experiments where the  $\lambda = 221$  nm photolyzed isoxazole matrix (containing a mixture of isoxazole and its photoproducts) was subjected to irradiations with  $\lambda \geq 240$  nm. Irradiation in the  $330 \leq \lambda \leq 340$  nm range induced direct transformation of 2-formyl-2H-azirine into 3-formylketenimine; irradiations with  $310 \leq \lambda \leq 318$  nm induced transformation of 3-formylketenimine into 3-hydroxypropenenitrile and imidoylketene; and irradiations with  $\lambda = 280$  nm and  $\lambda = 240$  nm permitted identification of 3-oxopropanenitrile, in the last case at the expense of 3-hydroxypropenenitrile tautomerization.

Several important mechanistic considerations were extracted from the observations: (i) photodecomposition of isoxazole to ketene and hydrogen cyanide seems to occur via an isoxazole carbene tautomer, formed by a [1,2] sigmatropic H-shift from isoxazole C5 to C4, and subsequent cleavage of the weakest N–O and C4–C3 bonds; (ii) the 2-formyl-2H-azirine and 3-formylketenimine are primary isomerization products in the isoxazole photochemistry, both species presumably resulting from rearrangements of an initially formed vinylnitrene in its excited open-shell singlet and ground triplet states, respectively; (iii) the vibrationally excited triplet vinylnitrene seems also to be involved in the observed conversion of 2-formyl-2H-azirine into 3-formylketenimine, via Curtius-like rearrangement, upon irradiation in the  $330 \leq \lambda \leq 340$  nm range; (iv) on the other hand, the nonobservation of oxazole indicates that under these conditions the 2H-azirine does not react via C–C bond cleavage; (v) photoisomerization of 3-formylketenimine to hydroxynitrile and imidoylketene was observed for the first time; and finally, (vi) observation of phototautomerization of the hydroxynitrile to the corresponding ketonitrile, upon irradiation at  $\lambda = 240$  nm, suggests that this reaction should take place preferentially with 5-unsubstituted isoxazoles, where the required [1,5] sigmatropic H-shift from ketenimine to hydroxynitrile is not blocked and the subsequent phototautomerization to ketonitriles can occur.



#### 4. EXPERIMENTAL SECTION

**Sample.** A commercial sample of isoxazole 1 (Aldrich, 99% purity) was used.

**Matrix-Isolation FTIR Spectroscopy.** Prior to usage, the sample was degassed by using the standard freeze–pump–thaw method. The sample vapor was premixed with high purity argon (N60, supplied by Air Liquide), in ratios from 1:1000 to 1:2000, using standard monomeric techniques. The matrices were prepared by effusive deposition of the premixed samples, from a 3 L glass reservoir, and the flux was controlled by reading the drop pressure in the reservoir. A CsI window, cooled to 15 K, was used as an optical substrate for the matrices. The temperature of the CsI window was measured directly by a silicone diode sensor connected to a digital controller with accuracy of  $\pm 0.1$  K. In all experiments, an APD Cryogenics closed helium refrigeration system with DE-202A expander was used.

The IR spectra were obtained using a Fourier transform infrared spectrometer, equipped with a deuterated triglycine sulfate (DTGS) detector and a Ge/KBr beam splitter, with  $0.5\text{ cm}^{-1}$  resolution. To avoid interference from atmospheric  $\text{H}_2\text{O}$  and  $\text{CO}_2$ , the optical path of the spectrometer was continuously purged by a stream of dry air.

**UV-Laser Irradiation Experiments.** The matrices were irradiated through an outer quartz window of the cryostat, using a frequency-doubled signal beam provided by a MOPO-SL optical parametric oscillator (fwhm  $\sim 0.2\text{ cm}^{-1}$ , repetition rate = 10 Hz, pulse energy  $\sim 1$  mJ, duration = 10 ns) pumped with a pulsed Nd:YAG laser.

**Theoretical Calculations.** All calculations were performed with Gaussian 03<sup>75</sup> at MP2<sup>76</sup> and DFT levels of theory using the standard 6-311++G(d,p) basis set.<sup>77,78</sup> The DFT calculations were carried out with the three-parameter density functional B3LYP,<sup>79</sup> which includes Becke's gradient exchange correction,<sup>80</sup> the Lee, Young, Parr,<sup>81</sup> and the Vosko, Wilk, Nusair correlation functionals.<sup>82</sup> The geometry optimizations were followed by harmonic frequency calculations, at the same level of theory, which also allowed characterization of the nature of the stationary points. To correct for the vibrational anharmonicity, basis set truncation, and the neglected part of electron correlation, the calculated frequencies below  $3100\text{ cm}^{-1}$  were scaled down by 0.980 (B3LYP) or 0.976 (MP2) and by 0.950 if they are above  $3100\text{ cm}^{-1}$ . The resulting frequencies, together with the calculated intensities, were used to simulate the spectra shown in the figures by convoluting each peak with a Lorentzian function with a full width at half-maximum (fwhm) of  $2\text{ cm}^{-1}$ .<sup>83</sup> Note that the peak intensities in the simulated spectra (arbitrary units of "relative intensity") are several times less than the calculated intensities (in  $\text{km mol}^{-1}$ ).

#### ■ ASSOCIATED CONTENT

##### ■ Supporting Information

Tables listing the observed IR peaks and their assignment based on MP2 or B3LYP calculations or experimental reported data, for ketene 2, hydrogen cyanide 3, 3-formylketenimine 5, 2-formyl-2H-azirine 4, and 3-hydroxypropenenitrile 6. IR spectra from laser irradiation isoxazole 1 with  $\lambda = 221\text{ nm}$  at different times. PES profile for internal rotation of the C–C bond of 2-formyl-2H-azirine 4, 3-formyl-N-ketenimine 5, and 3-oxopropanenitrile 8. Calculated relative energies for the different conformations of 3-hydroxypropenenitrile 6 and imidoalkene 7. Cartesian coordinates and frequencies (2–8) from MP2/6-311++G(d,p) and (4–5) from B3LYP/6-311++G(d,p). This material is available free of charge via the Internet at <http://pubs.acs.org>.

#### ■ AUTHOR INFORMATION

##### Corresponding Author

\*E-mail: [cmnunes@qui.uc.pt](mailto:cmnunes@qui.uc.pt); [reva@qui.uc.pt](mailto:reva@qui.uc.pt).

##### Notes

The authors declare no competing financial interest.

#### ■ ACKNOWLEDGMENTS

These studies were partially funded by the Portuguese "Fundação para a Ciência e a Tecnologia" (FCT), FEDER, and projects PTDC/QUI-QUI/111879/2009 and PTDC/QUI-QUI/118078/2010, FCOMP-01-0124-FEDER-021082, cofunded by QREN-COMPETE-UE. C. M. Nunes acknowledges FCT for Grant No. SFRH/BD/28844/2006 and I. Reva for Grant No. IF/00464/2012. We thank Prof. Hugh Douglas Burrows for the helpful discussions.

#### ■ REFERENCES

- (1) *Comprehensive Heterocyclic Chemistry*; Lang, S. A., Lin, Y. I., Eds.; Pergamon: Oxford, 1984; Vol. 6, Part 4B.
- (2) *Chemistry of Heterocyclic Compounds*; Grünanger, P., Vita-Finzi, P., Eds.; John Wiley and Sons: New York, 1991; Vol. 49, Part 1.
- (3) *Comprehensive Heterocyclic Chemistry III*; Gomi, D., Cordero, F. M., Machetti, F., Eds.; Elsevier: Oxford, 2008; p 365.
- (4) Pevarello, P.; Amici, R.; Brasca, M. G.; Villa, M.; Varasi, M. *Targets Heterocycl. Syst.: Chem. Prop.* **1999**, *3*, 301.
- (5) Pinho e Melo, T. M. V. D. *Curr. Org. Chem.* **2005**, *9*, 925.
- (6) Fonseca, S. M.; Burrows, H. D.; Nunes, C. M.; Pinho e Melo, T. M. V. D.; Gonsalves, A. M. d'A. R. *Chem. Phys. Lett.* **2005**, *414*, 98.
- (7) Fonseca, S. M.; Burrows, H. D.; Nunes, C. M.; Pinho e Melo, T. M. V. D. *Chem. Phys. Lett.* **2009**, *474*, 84.
- (8) Lopes, S.; Nunes, C. M.; Gómez-Zavaglia, A.; Pinho e Melo, T. M. V. D.; Fausto, R. *J. Phys. Chem. A* **2011**, *115*, 1199.
- (9) Nunes, C. M.; Reva, I.; Pinho e Melo, T. M. V. D.; Fausto, R.; Šolomek, T.; Bally, T. *J. Am. Chem. Soc.* **2011**, *133*, 18911.
- (10) Dalvie, D. K.; Kalgutkar, A. S.; Khojasteh-Bakht, S. C.; Obach, R. S.; O'Donnell, J. P. *Chem. Res. Toxicol.* **2002**, *15*, 269.
- (11) Kalgutkar, A. S.; Nguyen, H. T.; Vaz, A. D. N.; Doan, A.; Dalvie, D. K. *Drug Metab. Dispos.* **2003**, *31*, 1240.
- (12) Yu, J.; Folmer, J. J.; Hoesch, V.; Doherty, J.; Campbell, J. B.; Burdette, D. *Drug Metab. Dispos.* **2011**, *39*, 302.
- (13) Ullman, E. F.; Singh, B. *J. Am. Chem. Soc.* **1966**, *88*, 1844.
- (14) Singh, B.; Ullman, E. F. *J. Am. Chem. Soc.* **1967**, *89*, 6911.
- (15) Singh, B.; Zweig, A.; Gallivan, J. B. *J. Am. Chem. Soc.* **1972**, *94*, 1199.
- (16) D'Auria, M. *Adv. Heterocycl. Chem.* **2001**, *79*, 41.
- (17) Tanaka, H.; Osamura, Y.; Matsushita, T.; Nishimoto, K. *Bull. Chem. Soc. Jpn.* **1981**, *54*, 1293.
- (18) Good, R. H.; Jones, G. *J. Chem. Soc. C* **1971**, 1196.
- (19) Padwa, A.; Chen, E.; Ku, A. *J. Am. Chem. Soc.* **1975**, *97*, 6484.
- (20) Grellmann, K. H.; Tauer, E. *J. Photochem.* **1977**, *6*, 365.
- (21) Sauers, R. R.; Hadel, L. M.; Scimone, A. A.; Stevenson, T. A. *J. Org. Chem.* **1990**, *55*, 4011.
- (22) Kurtz, D. W.; Shechter, H. *Chem. Commun.* **1966**, 689.
- (23) Ferris, J. P.; Antonucci, F. R.; Trimmer, R. W. *J. Am. Chem. Soc.* **1973**, *95*, 919.
- (24) Sato, T.; Yamamoto, K.; Fukui, K. *Chem. Lett.* **1973**, 111.
- (25) Ferris, J. P.; Antonucci, F. R. *J. Am. Chem. Soc.* **1974**, *96*, 2014.
- (26) Heinzelmann, W.; Märky, M. *Helv. Chim. Acta* **1974**, *57*, 376.
- (27) Sato, T.; Saito, K. *J. Chem. Soc., Chem. Commun.* **1974**, 781.
- (28) Dietliker, K.; Gilgen, P.; Heimgartner, H.; Schmid, H. *Helv. Chim. Acta* **1976**, *59*, 2074.
- (29) Ferris, J. P.; Trimmer, R. W. *J. Org. Chem.* **1976**, *41*, 13.
- (30) Sato, T.; Yamamoto, K.; Fukui, K.; Saito, K.; Hayakawa, K.; Yoshiie, S. *J. Chem. Soc., Perkin Trans. 1* **1976**, 783.
- (31) Sauers, R. R.; Van Arnum, S. D. *Tetrahedron Lett.* **1987**, *28*, 5797.
- (32) Pavlik, J. W.; St. Martin, H.; Lambert, K. A.; Lowell, J. A.; Tsefrikas, V. M.; Eddins, C. K.; Kebede, N. *J. Heterocycl. Chem.* **2005**, *42*, 273.
- (33) Adembri, G.; Donati, D.; Ponticelli, F. *J. Photochem.* **1981**, *17*, 81.
- (34) Tidwell, T. T. *Spectroscopy and Physical Properties of Ketenes*. In *Ketenes II*, Second ed.; John Wiley and Sons: Hoboken, NJ, 2006.

- (35) Moore, C. B.; Pimentel, G. C. *J. Chem. Phys.* **1963**, *38*, 2816.
- (36) Romano, R. M.; Della Vedova, C. O.; Downs, A. J. *J. Phys. Chem. A* **2002**, *106*, 7235.
- (37) Breda, S.; Reva, I.; Fausto, R. *J. Phys. Chem. A* **2012**, *116*, 2131.
- (38) Milligan, D. E.; Jacox, M. E. *J. Chem. Phys.* **1967**, *47*, 278.
- (39) Satoshi, K.; Takayanagi, M.; Nakata, M. *J. Mol. Struct.* **1997**, *413*, 365.
- (40) Guennoun, Z.; Couturier-Tamburelli, I.; Combes, S.; Aycard, J. P.; Pietri, N. *J. Phys. Chem. A* **2005**, *109*, 11733.
- (41) The analysis of successive 1 min irradiation experiments of **1** ( $\lambda = 221$  nm) shows that some of the photoisomerization products reach their maxima during the first minutes, while others reach their maxima somewhat later (Figure S1, SI).
- (42) The first irradiation experiment ( $\lambda = 320$  nm, 1 min, Table S2, SI) of photoisomerization products of **1**, generated at  $\lambda = 221$  nm, led to the complete consumption of minor bands at 1915, 1657, and 868  $\text{cm}^{-1}$  which correspond to an unidentified species.
- (43) The photodecomposition products, ketene **2** and hydrogen cyanide **3**, do not react during irradiations with  $\lambda \geq 240$  nm.
- (44) Krantz, A.; Hoppe, B. *J. Am. Chem. Soc.* **1975**, *97*, 6590.
- (45) Briehl, H.; Lukosch, A.; Wentrup, C. *J. Org. Chem.* **1984**, *49*, 2772.
- (46) Wentrup, C.; Briehl, H.; Lorencak, P.; Vogelbacher, U. J.; Winter, H. W.; Maquestiau, A.; Flammang, R. *J. Am. Chem. Soc.* **1988**, *110*, 1337.
- (47) Bencheikh, A.; Chuche, J.; Manisse, N.; Pommelet, J. C.; Netsch, K. P.; Lorencak, P.; Wentrup, C. *J. Org. Chem.* **1991**, *56*, 970.
- (48) Kappe, C. O.; Kollenz, G.; Regis, L. T.; Wentrup, C. *J. Chem. Soc., Chem. Commun.* **1992**, 487.
- (49) Fulloon, B.; Elnabi, H. A. A.; Kollenz, G.; Wentrup, C. *Tetrahedron Lett.* **1995**, *36*, 6547.
- (50) Fulloon, B. E.; Wentrup, C. *J. Org. Chem.* **1996**, *61*, 1363.
- (51) Moloney, D. J. W.; Wong, M. W.; Flammang, R.; Wentrup, C. *J. Org. Chem.* **1997**, *62*, 4240.
- (52) George, L.; Bernhardt, P. V.; Netsch, K. P.; Wentrup, C. *Org. Biomol. Chem.* **2004**, *2*, 3518.
- (53) The imidoyleketene **7** is reported to be generated from pyrolysis of Meldrum's acid, and its identification was suggested only based on the observation of a band at 2130  $\text{cm}^{-1}$  at 77 K (neat) (ref 45). This band correlates well with the current observed band at 2136/2134  $\text{cm}^{-1}$ , which is attributed to *anti*-(*E*)-**7** isolated in the argon matrix.
- (54) The  $\nu(\text{C}\equiv\text{N})$  of ketonitrile *anti*-**8** was estimated, at the MP2 level, to have an infrared absorption at least 100 times less intense than the corresponding  $\nu(\text{C}=\text{O})$ , justifying in this way its nonobservation.
- (55) Kim, H. S.; Kim, K. *Bull. Korean Chem. Soc.* **1992**, *13*, 520.
- (56) Bernstein, M. P.; Sandford, S. A.; Allamandola, L. J. *Astrophys. J.* **1997**, *476*, 932.
- (57) Sechkarev, A. V.; Fadeev, Y. A.; Reva, I. D. *J. Appl. Spectrosc.* **1999**, *66*, 708.
- (58) Abe, H.; Takeo, H.; Yamada, K. M. T. *Chem. Phys. Lett.* **1999**, *311*, 153.
- (59) Abe, H.; Yamada, K. M. T. *Struct. Chem.* **2003**, *14*, 211.
- (60) The molecular modeling studies on the mechanism of the isoxazole-oxazole photoisomerization (the most common reaction in the isoxazole photochemistry) should be considered with care, if analyzed for the simplest parent isoxazole **1**, because this reaction was not observed under present experimental conditions (as described in this work).
- (61) Karney, W. L.; Borden, W. T. *J. Am. Chem. Soc.* **1997**, *119*, 1378.
- (62) Platz, M. S. *Nitrenes*, In *Reactive Intermediate Chemistry*; Moss, R. A., Platz, M. S., Maitland, J., Eds.; Wiley-Interscience: Hoboken, NJ, 2004.
- (63) Parasuk, V.; Cramer, C. J. *Chem. Phys. Lett.* **1996**, *260*, 7.
- (64) Albini, A.; Bettinetti, G.; Minoli, G. *J. Am. Chem. Soc.* **1997**, *119*, 7308.
- (65) Harder, T.; Stosser, R.; Wessig, P.; Bendig, J. *J. Photochem. Photobiol. A* **1997**, *103*, 105.
- (66) Murata, S.; Tsubone, Y.; Tomioka, H. *Chem. Lett.* **1998**, 549.
- (67) Inui, H.; Murata, S. *Chem. Lett.* **2001**, 832.
- (68) Inui, H.; Murata, S. *Chem. Commun.* **2001**, 1036.
- (69) Inui, H.; Murata, S. *J. Am. Chem. Soc.* **2005**, *127*, 2628.
- (70) Gómez-Zavaglia, A.; Kaczor, A.; Cardoso, A. L.; Pinho e Melo, T. M. V. D.; Fausto, R. *J. Phys. Chem. A* **2006**, *110*, 8081.
- (71) Kaczor, A.; Gómez-Zavaglia, A.; Cardoso, A. L.; Pinho e Melo, T. M. V. D.; Fausto, R. *J. Phys. Chem. A* **2006**, *110*, 10742.
- (72) Inui, H.; Murata, S. *Chem. Phys. Lett.* **2002**, *359*, 267.
- (73) Giuliano, B. M.; Reva, I.; Fausto, R. *J. Phys. Chem. A* **2010**, *114*, 2506.
- (74) Kuş, N.; Reva, I.; Fausto, R. *J. Phys. Chem. A* **2010**, *114*, 12427.
- (75) Frisch, M. J.; Trucks, G. W.; Schlegel, H. B. et al. *GAUSSIAN 03*, Revision C.02; Gaussian, Inc.: Wallingford, CT, 2004.
- (76) Head-Gordon, M.; Head-Gordon, T. *Chem. Phys. Lett.* **1994**, *220*, 122.
- (77) Frisch, M. J. P., J. A.; Binkley, J. S. *J. Chem. Phys.* **1984**, *80*, 3265.
- (78) Clark, T. C., J.; Spitznagel, G. W.; Schleyer, P. V. R. *J. Comput. Chem.* **1983**, *4*, 294.
- (79) Becke, A. D. *J. Chem. Phys.* **1993**, *98*, 5648.
- (80) Becke, A. D. *Phys. Rev. A* **1988**, *38*, 3098.
- (81) Lee, C.; Yang, W.; Parr, R. G. *Phys. Rev. B* **1988**, *37*, 785.
- (82) Vosko, S. H.; Wilk, L.; Nusair, M. *Can. J. Phys.* **1980**, *58*, 1200.
- (83) Irikura, K. K. *Program SYNSPEC*; Natl. Inst. Standards and Technol.: Gaithersburg, MD20899, USA.